Input Design for System Order Estimation ⋆

Mohammad Amin Sheikhi * **Gabriel de Albuquerque Gleizer** *
Peyman Mohajerin Esfahani *,** **Tamás Keviczky** *

* *Delft Center for Systems and Control, Delft University of Technology, Mekelweg 2, 2628 CD Delft, The Netherlands (e-mail: {m.a.sheikhi, g.gleizer, p.mohajerinesfahani, and t.keviczky}@tudelft.nl).*
** *Department of Mechanical and Industrial Engineering, University of Toronto, Toronto, Canada (e-mail: p.mohajerinesfahani@utoronto.ca)*

Abstract: Even though system identification of LTI systems is very well established, determining their true order based purely on data remains a notorious challenge. In this paper, we address this via a novel input design method, which consists of two loops. In the outer loop, a hypothesized system order r is tested in the real system through an input designed in the the inner loop. The input is designed to maximize the minimal singular value of the data matrices of the r-th order model approximation coming from standard identification methods. The design is enabled by a tractable optimization problem formulation that exploits the structure of the data, for which we propose an efficient first-order algorithm. We show that our proposed method not only increases the spectral gap used for order estimation, but also reduces identification error. Finally, numerical studies are provided to validate the effectiveness of the proposed method.

Keywords: Active learning and experiment design; Linear system identification; Data-driven control theory

1. INTRODUCTION

One of the most fundamental parameters of linear time-invariant systems is its order; yet, it is notoriously difficult to estimate it from raw input-output data. In fact, most identification methods either rely or dramatically benefit from the order being prior knowledge. For example, parametric identification methods generally require it as an input, while subspace methods circumvent this requirement by estimating the order of the system via a spectral gap analysis on relevant data matrices (Ljung, 1998; Verhaegen and Verdult, 2007). However, successfully determining the order is highly dependent on the experiment that generated the data. Standard randomized inputs such as pseudo-random binary sequences (PRBS) sometimes fail to excite the the right directions or dynamics to make them stand out against the noise, as reported for example by Misra and Nikolaou (2017).

Several theoretical results exist on experiment design in the absence of noise. Initially this was achieved by the seminal paper (Willems et al., 2005) and its persistency of excitation (PE) lemma: in the absence of noise and with the input satisfying PE conditions, the spectral gap analysis reduces to a rank computation, which retrieves the correct system order. This framework has been relaxed when the goal is control instead of complete identification (Yu et al., 2021). Classically, determining the order of an LTI system under noise is possible in the limit case of infinite data, by the consistency results in, e.g., (Verhaegen and Dewilde, 1992; Verhaegen and Verdult, 2007; Van Overschee and De Moor, 1994). In this limit case, the contribution of the noise vanishes in the spectral analysis. In the more realistic case of finite data, the qualitative notion of PE has been expanded to a quantitative version (Coulson et al., 2022), which finds sufficient conditions on the input power so that the order is distinguishable during the spectral analysis. Given that the order is known, a massive amount of literature covers experiment design in order to maximize the accuracy of the obtained parameters, see (Aoki and Staley, 1970; Goodwin, 1971; Mehra, 1974) for the early works and (Lindqvist and Hjalmarsson, 2001; Bombois et al., 2011; Dirkx et al., 2020; Wagenmaker and Jamieson, 2020) for an incomprehensive list of more recent developments.

So far, the literature lacks a systematic method to design optimally exciting inputs to obtain the correct order of an LTI system in the presence of noise, in the realistic case of limited data availability from controlled experiments. In this work, we propose a method of designing a series of experiments to determine the order of an LTI system subject to noise. For that, we build on the subspace approach for model order determination, which is a spectral gap analysis. The method relies on the principle that input can be designed to both *confirm a model order* and *falsify a model order*. Given an input that improves the spectral gap for a given model, this improvement should also be reflected in the real system if the order is right. If the model order is larger than the real system's, no statistically

⋆ This work was partially supported by the Digital Twin project with project number P18-03 of the research programme TTW-Perspective which is (partly) financed by the Dutch Research Council (NWO).

relevant improvement in the spectral gap should be seen. To realize this method, we develop a first-order algorithm to design inputs that maximize the spectral gap given a model. We test our method on a simple example that already showcases the difficulty of using spectral analysis for order determination under random inputs. Our method consistently determines the right order of the system, and also results in a more identification than that obtained from the baseline random input. Moreover, despite solving an inherently non-convex optimization problem, our input design algorithm is remarkably fast and stable, making it potentially useful as a tool on its own.

Notation. We denote by $\mathbb{R}$ the set of real numbers. The convex hull of a set $\mathcal{Z}$ is denoted by $\operatorname{conv}(\mathcal{Z})$. The Euclidean norm of a vector $\boldsymbol{z}$ is denoted by $\|\boldsymbol{z}\|$. Let $\boldsymbol{I}$ denote the identity matrix, where $\boldsymbol{I}_n$ specifies its size n. Given a matrix $\boldsymbol{Z} \in \mathbb{R}^{n\times m}$, we denote by $\boldsymbol{Z}^\mathsf{T}$ its transpose, by $\operatorname{SVD}(\boldsymbol{Z})$ its singular value decomposition $\boldsymbol{U\Sigma V}^\mathsf{T}$, by $\sigma_k(\boldsymbol{Z})$ its k-th largest singular value, and by $\operatorname{vec}(\boldsymbol{Z})$ its vectorization. The notations $\mathbf{Z}$, $\mathbf{Z}$, and $\mathbf{Z}$ imply its Hankel, lower-triangular block Toeplitz and upper-triangular block Toeplitz structures, respectively. The diagonal matrix built from a vector $\boldsymbol{z}$ is denoted by $\operatorname{diag}(\boldsymbol{z})$. From a sequence $\{\boldsymbol{z}_i\}_{i=0}^{N-1}$, we denote by $\boldsymbol{z}_{[0,N-1]} := \begin{bmatrix}\boldsymbol{z}_0^\mathsf{T} & \cdots & \boldsymbol{z}_{N-1}^\mathsf{T}\end{bmatrix}^\mathsf{T}$ the vector built by vertically stacking $\boldsymbol{z}_i$, and its block-Hankel form by

$$\mathbf{Z}_{k,L,N} := \begin{bmatrix} \boldsymbol{z}_k & \boldsymbol{z}_{k+1} & \cdots & \boldsymbol{z}_{k+N-L} \\ \boldsymbol{z}_{k+1} & \boldsymbol{z}_{k+2} & \cdots & \boldsymbol{z}_{k+N-L+1} \\ \vdots & \vdots & \ddots & \vdots \\ \boldsymbol{z}_{k+L-1} & \boldsymbol{z}_{k+L} & \cdots & \boldsymbol{z}_{k+N-1} \end{bmatrix}.$$

2. PROBLEM STATEMENT

2.1 Setup and preliminaries

Consider a finite-dimensional discrete-time LTI system subject to additive noise described as

$$\begin{aligned} \boldsymbol{x}_{k+1} &= \boldsymbol{A}\boldsymbol{x}_k + \boldsymbol{B}\boldsymbol{u}_k\,, \\ \boldsymbol{y}_k &= \boldsymbol{C}\boldsymbol{x}_k + \boldsymbol{D}\boldsymbol{u}_k + \boldsymbol{e}_k\,. \end{aligned} \tag{1}$$

where $\boldsymbol{x}_k \in \mathbb{R}^{n_x}$, $\boldsymbol{u}_k \in \mathbb{R}^{n_u}$, $\boldsymbol{y}_k \in \mathbb{R}^{n_y}$, and $\boldsymbol{e}_k \in \mathbb{R}^{n_y}$ denote the system states, input (control) signal, output signal, and additive measurement noise, respectively. The quadruple $(\boldsymbol{A},\boldsymbol{B},\boldsymbol{C},\boldsymbol{D})$ is the state-space realization with compatible dimensions. The additive noise $\boldsymbol{e}_k$ is zero-mean, independent and identically distributed (i.i.d) white noise with variance ε_e^2, and is statistically independent of the input signal $\boldsymbol{u}_k$. The corresponding Markov parameters are given by

$$\boldsymbol{M}_i = \begin{cases} \boldsymbol{D} & i = 0 \\ \boldsymbol{C}\boldsymbol{A}^{i-1}\boldsymbol{B} & i > 0 \end{cases}.$$

Assumption 2.1. (Minimal Realization). The system (1) admits a minimal realization of order n, meaning that the state dimension satisfies $n_x = n$.

The first step in any subspace identification method requires the estimation of system's minimal order or the McMillan degree. To this end, we collect input–output (I/O) data points $\mathcal{D} := \{\boldsymbol{u}_i, \boldsymbol{y}_i\}_{i=0}^{N-1}$ generated according to the system (1), which are the only measurable signals (states cannot be measured directly). Consequently, the data collected over $[0, N-1]$ can be arranged into the following Hankel form

$$\mathbf{Y}_{0,L,N} = \mathbf{O}_L\mathbf{X}_{0,1,N} + \mathbf{M}_L\mathbf{U}_{0,L,N} + \mathbf{E}_{0,L,N}\,,$$

where the extended observability $\mathbf{O}_L$ and the lower-triangular block-Toeplitz matrix of Markov parameters $\mathbf{M}_L$ are defined as

$$\mathbf{O}_L := \begin{bmatrix} \boldsymbol{C} \\ \boldsymbol{CA} \\ \vdots \\ \boldsymbol{CA}^{L-1} \end{bmatrix}, \quad \mathbf{M}_L := \begin{bmatrix} \boldsymbol{M}_0 & 0 & \cdots & 0 \\ \boldsymbol{M}_1 & \boldsymbol{M}_0 & \ddots & \vdots \\ \vdots & \ddots & \ddots & 0 \\ \boldsymbol{M}_{L-1} & \cdots & \boldsymbol{M}_1 & \boldsymbol{M}_0 \end{bmatrix}.$$

In subspace identification, one typically reconstructs the column space of $\mathbf{O}_L$, $\operatorname{col}(\mathbf{O}_L)$, from the recorded data $\mathcal{D}$. For a minimal system (1), $\operatorname{rank}(\mathbf{O}_L) = n$. This implies that the system order is directly linked to the dimension of $\operatorname{col}(\mathbf{O}_L)$. We briefly revisit the fundamentals of system order determination to set the stage for the main result (Van Overschee and De Moor, 1994; Verhaegen and Verdult, 2007).

To estimate $\operatorname{col}(\mathbf{O}_L)$, a suitable linear transformation $\boldsymbol{P}_\mathcal{D}$ can be found that maps $\mathbf{Y}_{0,L,N}$ into a subspace preserving the information on the column space of observability. While the specific form of this transformation varies across subspace identification methods, the underlying idea remains the same. For example, the N4SID method (Van Overschee and De Moor, 1994) employs an oblique projection to define $\boldsymbol{P}_\mathcal{D}$, whereas the MOESP approach uses an orthogonal projection for this purpose (Verhaegen and Dewilde, 1992). The next assumption on the data set is required to ensure that $\operatorname{col}(\mathbf{O}_L)$ remains recoverable after the transformation.

Assumption 2.2. (Data Rank Condition). The data is recorded such that the following holds:

$$\operatorname{rank}\begin{bmatrix} \mathbf{X}_{0,1,N} \\ \mathbf{U}_{0,L,N} \end{bmatrix} = Ln_u + n$$

Although Assumption 2.2 is general, it can be guaranteed under certain practical conditions, namely: 1) the input signal is persistently exciting (PE) of sufficient order, and 2) the system operates in open-loop, or, in the closed-loop case, the feedback loop contains at least a unit delay. A time-domain description of PE for a signal is provided as follows (Willems et al., 2005).

Definition 2.1. (Persistently Exciting). A signal $\boldsymbol{u}_k$ for k in time interval $[0, N-1]$ is persistently exciting of order L if its Hankel matrix has full row rank, i.e.,

$$\operatorname{rank}(\mathbf{U}_{0,L,N}) = Ln_u\,.$$

The fundamental lemma states that an input $\boldsymbol{u}_{[0,N-1]}$ with PE of order $L + n$ is sufficient to ensure that Assumption 2.2 is satisfied [ref, Willems' lemma]. Additionally, under the ergodicity of the process, the following holds:

$$\mathbb{E}\left[(\mathbf{Y}_{0,L,N}\boldsymbol{P}_\mathcal{D})\right] = \lim_{N\to\infty}\frac{1}{N}(\mathbf{Y}_{0,L,N}\boldsymbol{P}_\mathcal{D})$$

Suppose the data is collected such that Assumption 2.2 is satisfied. Then, it can be shown that, as $N \to \infty$, the compact singular value decomposition (SVD) of $\mathbf{Y}_{0,L,N}\boldsymbol{P}_{\mathcal{D}}$ takes the form

$$\mathrm{SVD}\left(\lim_{N\to\infty}\frac{1}{N}(\mathbf{Y}_{0,L,N}\boldsymbol{P}_{\mathcal{D}})\right) = \left[\boldsymbol{Q}_n \ \boldsymbol{Q}_{\bar{n}}^{\mathsf{T}}\right]\begin{bmatrix}\sqrt{\Sigma_n^2+\varepsilon_e^2\boldsymbol{I}} & \mathbf{0}\\ \mathbf{0} & \varepsilon_e\boldsymbol{I}\end{bmatrix}\begin{bmatrix}\boldsymbol{V}_n^{\mathsf{T}}\\ \boldsymbol{V}_{\bar{n}}^{\mathsf{T}}\end{bmatrix} \tag{2}$$

From this decomposition, one can observe that the underlying system information is captured by ($\boldsymbol{Q}_n$, $\sqrt{\Sigma_n^2+\varepsilon_e^2\boldsymbol{I}}$, $\boldsymbol{V}_n$). In this representation, $\mathrm{col}(\mathbf{O}_L) = \mathrm{col}(\boldsymbol{Q}_n)$, indicating that the number of nonzero singular values contained in the block $\sqrt{\Sigma_n^2+\varepsilon_e^2\boldsymbol{I}}$ reveals the system order. However, since all singular values are perturbed by noise, a singular-value inspection is required to recover the true separation. Under a sufficiently high signal-to-noise ratio (SNR), a significant drop, often exhibiting an 'elbow' shape, is expected at n, thereby indicating the true order. Once the system order n is determined, the state-space realization matrices $(\boldsymbol{A}, \boldsymbol{B}, \boldsymbol{C}, \boldsymbol{D})$ can be estimated using the existing subspace identification methods (Van Overschee and De Moor, 1994; Verhaegen and Dewilde, 1992). However, as previously discussed, a clear separation in the spectrum is not always guaranteed, as it depends on several factors, including system properties, the input signal, and noise perturbations, making order estimation a challenging task. Moreover, the corresponding SVD (2) is only valid asymptotically ($N \to \infty$), whereas in practice we are restricted to finite samples. To illustrate these challenges, we provide an example in the subsequent section.

2.2 Motivating Example

In this subsection, synthetic data are generated according to the system (1) with minimal order $n = 3$. The data set $\mathcal{D}$ consists of $N = 100$ samples with a SNR of approximately 10, satisfying Assumption 2.2. Following standard subspace identification methods, we plot the singular values on a logarithmic scale to identify the significant drop in the spectrum. Before discussing the results, it is worth noting that, in addition to the aforementioned MOESP and N4SID approaches, there exists another way to observe the drop in the singular values. Under Assumption 2.2, the singular values of the augmented Hankel matrix of input–output data $\mathbf{W}_L$ also demonstrates a similar spectral pattern, that is,

$$\mathrm{SVD}(\mathbf{W}_L); \quad \mathbf{W}_L := \begin{bmatrix}\mathbf{U}_{0,L,N}\\ \mathbf{Y}_{0,L,N}\end{bmatrix}. \tag{3}$$

However, instead of occurring at the n-th largest singular value, the drop appears at Ln_u+n. Using MOESP, N4SID and augmented Hankel for revealing the system order, we first present the results for the noise-free condition in Figure 1a. Subsequently, the results for the noisy condition are shown in Figure 1b. While the drop occurs at the correct index in the noise-free case, the noisy case is noticeably affected by perturbations. In particular, for the MOESP and N4SID approaches, the drop appears at an earlier index ($i = 3$), which leads to an underestimation of the system order. The situation is even more problematic for the augmented Hankel technique. Therefore, the central question is whether there exists a way to improve the discrepancy in the singular values. Unlike the intrinsic system properties and the underlying noise, the input signal represents an available degree of freedom that can be designed, provided that experiment design is permissible.

2.3 Problem statement

In this work, we propose a method for generating input sequences that enhance the separability of singular values with respect to the true order of the system. Given an unknown finite-order system of the form 1, design a finite collection of input signals $\{\boldsymbol{u}_i\}_{i=0}^{N-1}$ of length N such that the true order of the system is determined.

Remark 1. (Bounded input). Naturally, the largest the power the input can have, the larger the SNR of the output will be. Hence, to make the problem well posed (and realistic), we also impose a limited power to the inputs that can be designed.

3. PROPOSED METHOD

In this section we present our main contribution: a method to generate a succession of experiments to determine the order of the unknown system (1). The method is composed of an outer loop and an inner loop. The inner loop (Section 3.1) generates optimized inputs for the next experiment, given information from the previous experiment. The outer loop (Section 3.2) executes experiments using the input generated in the inner loop and decides whether (i) the system order has been established, or (ii) if a new experiment is needed. This decision is based on the following pair of principles:

- **Input design to confirm the order.** Suppose system (1) has order $n \geq r$, and consider its r-th order approximation obtained from any system identification method. If an input sequence $\{\boldsymbol{u}\}_{i=0}^{N-1}$ can improve the the (Ln_u+r)-th largest singular value of the Hankel matrix $\mathbf{W}_L$, then the corresponding singular value coming from real data should also attain a similar improvement. This is because the r-th order dynamics do exist and can be excited by the designed input.
- **Input design to falsify the order.** Conversely, suppose system (1) has order $n < r$, and consider its r-th order model obtained via system identification. Any input sequence $\{\boldsymbol{u}\}_{i=0}^{N-1}$ that improves $\sigma_{Ln_u+r}(\mathbf{W}_L)$ should not make any statistically significant change in the corresponding singular value coming from real data. This is because the r-th mode identified is inexistent, and $\sigma_{Ln_u+r}(\mathbf{W}_L)$ from real data only captures spurious correlations between input and noise.

3.1 Optimal Input Design

The inner loop receives a model of order r, and its goal is to design an input that maximizes the spectral gap for this model. We propose an optimal input design aimed at maximizing the (Ln_u+r)-th singular value of the matrix $\mathbf{W}$ generated by the model.

Since the primary degree of freedom in input design is the input signal itself, we express the output as an explicit function of the input in the first step: in addition to $\mathbf{T}_L\mathbf{U}_{0,L,N}$ in (2.1), the state sequence $\mathbf{X}_{0,1,N}$ also contains contributions from $\boldsymbol{u}_k$. To make this explicit, we expand the state sequence as follows:

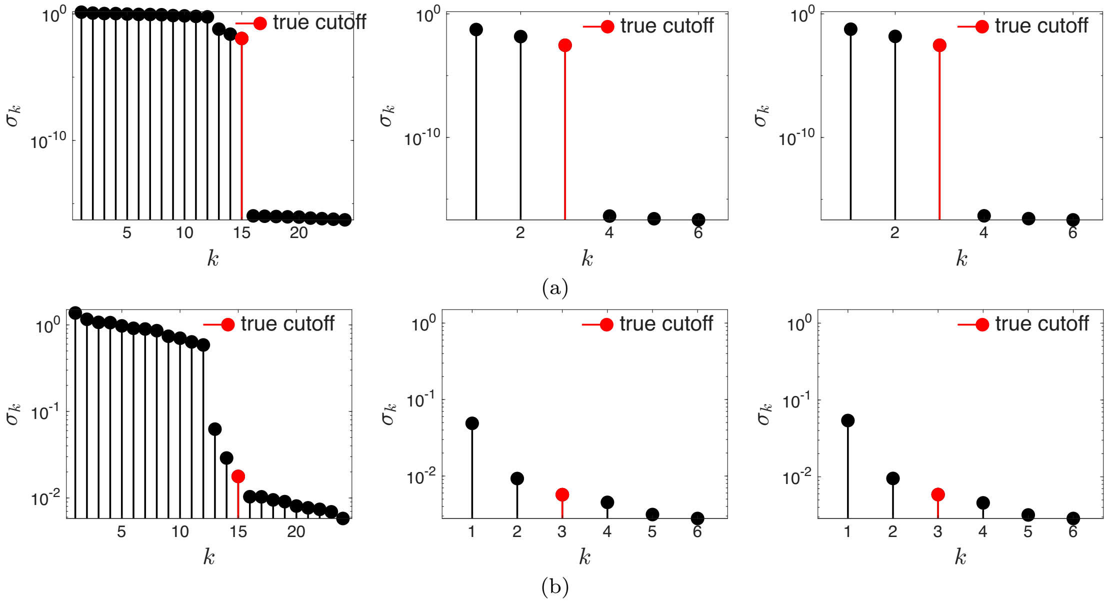

Fig. 1. From left to right column, each pair corresponds to the augmented Hankel of input-output data, MOESP (Verhaegen and Dewilde, 1992), and N4SID (Van Overschee and De Moor, 1994) methods. The singular values of the respective matrices, obtained using the order-revealing technique, are shown as black circles for the noise-free case in (a) and for the noisy case in (b). The ground-truth cutoff is indicated by a red circle, with its position depending on the method.

$$\tilde{\mathbf{X}}_{0,1,N} = \underbrace{\begin{bmatrix}\boldsymbol{I}_n & \boldsymbol{A} & \boldsymbol{A}^2 & \cdots & \boldsymbol{A}^{N-L}\end{bmatrix}}_{=:\bar{\mathbf{A}}_L}(\boldsymbol{I}_{N-L}\otimes \boldsymbol{x}_0) + \begin{bmatrix}\mathbf{0} & \boldsymbol{B}\boldsymbol{u}_0 & [\boldsymbol{AB}\ \boldsymbol{B}]\begin{bmatrix}\boldsymbol{u}_0\\ \boldsymbol{u}_1\end{bmatrix} & [\boldsymbol{A}^2\boldsymbol{B}\ \boldsymbol{AB}\ \boldsymbol{B}]\begin{bmatrix}\boldsymbol{u}_0\\ \boldsymbol{u}_1\\ \boldsymbol{u}_2\end{bmatrix} & \cdots\end{bmatrix}.$$

Using this expansion, the term $\mathbf{O}_L\tilde{\mathbf{X}}_{0,1,N}$ turns out to admit an interesting representation as a function of the input sequence:

$$\mathbf{O}_L\tilde{\mathbf{X}}_{0,1,N} = \mathbf{O}_L\bar{\mathbf{A}}_L(\boldsymbol{I}_{N-L}\otimes \boldsymbol{x}_0) + \tilde{\mathbf{M}}_{1,L,N-1}\begin{bmatrix}\mathbf{0} & \check{\mathbf{U}}_{N-L}\end{bmatrix}, \tag{4}$$

where the block-Hankel matrix of Markov parameters, $\tilde{\mathbf{M}}_{1,L,N-1}$, is defined as follows:

$$\tilde{\mathbf{M}}_{1,L,N-1} \coloneqq \begin{bmatrix}\boldsymbol{M}_1 & \boldsymbol{M}_2 & \cdots & \boldsymbol{M}_{N-L}\\ \boldsymbol{M}_2 & \boldsymbol{M}_3 & \cdots & \boldsymbol{M}_{N-L+1}\\ \vdots & \vdots & & \vdots\\ \boldsymbol{M}_L & \boldsymbol{M}_{L+1} & \cdots & \boldsymbol{M}_{N-1}\end{bmatrix},$$

and the upper-triangular block-Toeplitz matrix of input sequence, $\check{\mathbf{U}}_{N-L}$, is given by

$$\check{\mathbf{U}}_{N-L} \coloneqq \begin{bmatrix}\boldsymbol{u}_0 & \boldsymbol{u}_1 & \cdots & \boldsymbol{u}_{N-L-1}\\ \mathbf{0} & \boldsymbol{u}_0 & \cdots & \boldsymbol{u}_{N-L-2}\\ \vdots & \ddots & \ddots & \vdots\\ \mathbf{0} & \cdots & \mathbf{0} & \boldsymbol{u}_0\end{bmatrix}.$$

Using (4), the augmented Hankel matrix of input–output sequences in $\mathcal{D}$ can be expressed through the following equalities:

$$\begin{aligned}\begin{bmatrix}\tilde{\mathbf{U}}_{0,L,N}\\ \tilde{\mathbf{Y}}_{0,L,N}\end{bmatrix} &= \begin{bmatrix}\mathbf{0} & \boldsymbol{I}_{Ln_u}\\ \mathbf{O}_L & \check{\mathbf{M}}_L\end{bmatrix}\begin{bmatrix}\tilde{\mathbf{X}}_{0,1,N}\\ \tilde{\mathbf{U}}_{0,L,N}\end{bmatrix} + \begin{bmatrix}\mathbf{0}\\ \tilde{\mathbf{E}}_{0,L}\end{bmatrix},\\ &= \begin{bmatrix}\mathbf{0} & \boldsymbol{I}_{Ln_u}\\ \boldsymbol{I}_{Ln_y} & \check{\mathbf{M}}_L\end{bmatrix}\left(\begin{bmatrix}\mathbf{O}_L\bar{\mathbf{A}}_L(\boldsymbol{I}_{N-L}\otimes \boldsymbol{x}_0)\\ \mathbf{0}\end{bmatrix} + \begin{bmatrix}\tilde{\mathbf{M}}_{1,L,N-1}\begin{bmatrix}\mathbf{0} & \check{\mathbf{U}}_{N-L}\end{bmatrix}\\ \tilde{\mathbf{U}}_{0,L,N}\end{bmatrix}\right) + \begin{bmatrix}\mathbf{0}\\ \tilde{\mathbf{E}}_{0,L}\end{bmatrix}.\end{aligned}$$

After some mathematical manipulations, the final expression takes the following form

$$\mathbf{W}_L = \begin{bmatrix}\tilde{\mathbf{U}}_{0,L,N}\\ \tilde{\mathbf{Y}}_{0,L,N}\end{bmatrix} = \underbrace{\begin{bmatrix}\mathbf{0}\\ \mathbf{O}_L\bar{\mathbf{A}}_L(\boldsymbol{I}_{N-L}\otimes \boldsymbol{x}_0)\end{bmatrix}}_{\boldsymbol{\Xi}_0} + \underbrace{\begin{bmatrix}\mathbf{0} & \boldsymbol{I}_{Ln_u}\\ \tilde{\mathbf{M}}_{1,L,N-1} & \check{\mathbf{M}}_L\end{bmatrix}}_{\boldsymbol{F}}\underbrace{\begin{bmatrix}\mathbf{0}\ \check{\mathbf{U}}_{N-L}\\ \tilde{\mathbf{U}}_{0,L,N}\end{bmatrix}}_{\boldsymbol{\Theta}(\boldsymbol{u}_{[0,N-1]})} + \underbrace{\begin{bmatrix}\mathbf{0}\\ \tilde{\mathbf{E}}_{0,L}\end{bmatrix}}_{\boldsymbol{E}(\boldsymbol{e}_{[0,N-1]})}. \tag{5}$$

This representation offers two advantages: first, the contribution of input signal is completely encompassed in the $\boldsymbol{F\Theta}$; second, it shows that the matrices $\boldsymbol{\Xi}_0$ and $\boldsymbol{E}$ depend only on the initial condition and the noise perturbation, respectively, and not on the input signal. Since the optimization is performed in the model, no noise is present and the initial state can be selected zero, giving $\boldsymbol{\Xi}_0 = \boldsymbol{E} = \mathbf{0}$. Therefore, $\mathbf{W}_L$ only retains the component linear in $\boldsymbol{u}$.

Our proposed optimization problem is given by

$$\boldsymbol{u}^*_{[0,N-1]} \coloneqq \underset{\boldsymbol{u}_{[0,N-1]}\in\mathcal{U}}{\arg\max}\ \ \ell_r; \quad \ell_r \coloneqq \sigma_r(\mathbf{W}_L), \tag{6}$$

where the input set $\mathcal{U}$ for bounded-energy signals is defined as

$$\mathcal{U}(\gamma_u) := \{\boldsymbol{u}_{[0,N-1]} \in \mathbb{R}^{Nn_u} \,:\, \sum_{i=0}^{N-1} \boldsymbol{u}_i^\mathsf{T}\boldsymbol{u}_i \leq \gamma_u^2\}\,.$$

The original optimization (6) can be reformulated using (5)

$$\begin{aligned} \boldsymbol{\Theta}^* := \quad & \underset{\|\boldsymbol{u}(\boldsymbol{\Theta})\| \leq \gamma_\theta}{\arg\max} \quad \sigma_r\left(\boldsymbol{F}\boldsymbol{\Theta}\right) \\ & \text{subject to } \boldsymbol{\Pi}\,\mathrm{vec}(\boldsymbol{\Theta}) = \boldsymbol{0}\,. \end{aligned} \tag{7}$$

In this reformulation, the specific structure of the matrix $\boldsymbol{\Theta} \in \mathbb{R}^{Nn_u \times (N-L+1)}$ is enforced by the matrix $\boldsymbol{\Pi}$ through a set of linear constraints; namely, (i) setting the block-diagonal elements of $\overset{\diagdown}{\mathbf{U}}_{N-L}$ to be equal, (ii) setting the block-antidiagonal elements of $\overset{\diagup}{\mathbf{U}}_{0,L,N}$ to be equal, and (iii) setting the remaining elements to zero. Since $\boldsymbol{\Theta} \in \mathbb{R}^{Nn_u \times (N-L+1)}$ satisfies the structure, a unique $\boldsymbol{u}$ can be determined from it by using the first column and last row of $\overset{\diagup}{\mathbf{U}}_{0,L,N}$, thereby enabling the power constraint.

The cost function ℓ_r is generally non-concave and non-smooth. Consequently, maximizing a constrained non-concave problem is prone to convergence to a local optimum. Nevertheless, we can still employ a gradient ascent-based method to solve the optimization problem in (7), since the subgradient of the cost function has a closed-form solution. Applying the chain rule together with the susbgradient of a singular value yields to the following subgradient of the cost function at $\boldsymbol{\Theta}$:

$$\nabla\ell_r := \boldsymbol{F}^\mathsf{T}(\boldsymbol{q}_r\boldsymbol{v}_r^\mathsf{T})\,, \tag{8}$$

where $\boldsymbol{q}_r$ and $\boldsymbol{v}_r$ denote the left and right singular vectors corresponding to the r-th largest singular value of the SVD in (3).

Remark 3.1. The cost function in (7) is non-differentiable when the r-th largest singular value σ_r has multiplicity $m > 1$. In this general case, the subdifferential $\partial\ell_r$ at $\boldsymbol{\Theta}$ can be computed as (Lewis and Sendov, 2005, Thm. 7.1)

$$\begin{aligned} \partial\ell_r &:= \mathrm{conv}\left\{\boldsymbol{F}^\mathsf{T}(\boldsymbol{q}\boldsymbol{v}^\mathsf{T}) \,:\, \mathbf{W}_L\boldsymbol{v} = \sigma_r\boldsymbol{q}\right\}\,, \qquad (9)\\ &= \left\{\boldsymbol{F}^\mathsf{T}(\boldsymbol{Q}\,\mathrm{diag}(\boldsymbol{\alpha})\boldsymbol{V}^\mathsf{T}) \,:\, \mathbf{W}_L\boldsymbol{V} = \sigma_r\boldsymbol{Q},\ \sum_{i=1}^{m}\alpha_i = 1\right\}\,, \end{aligned}$$

in which $\boldsymbol{\alpha} := [\alpha_1, \ldots, \alpha_m]^\mathsf{T}$ is a vector of positive scalar components, i.e., $\alpha_i \geq 0$. All left and right singular vectors associated with σ_r are collected in $\boldsymbol{Q}$ and $\boldsymbol{V}$, respectively. The subgradient in (8) belongs to this set, hence it can be used even at points of non-differentiability.

The problem in (6) can be solved using Algorithm 1, which provides the function `OptimalInput`.

Algorithm 1 receives a model in state-space form and its corresponding matrix $\boldsymbol{F}$, see (5). Additionally, it receives an initial input sequence $\boldsymbol{u}_{[0,N-1]}$ and iterates over it. By applying this input to the model (Line 5), the matrix $\mathbf{W}_L$ is built and its singular value decomposition is computed (Line 6). From this and the matrix $\boldsymbol{F}$, the subgradient (8) is computed (Line 7); diminishing step sizes are chosen due to the non-smooth nature of the problem. Lines 8–12 perform a projected subgradient step: Line 8 starts with a standard subgradient step. This is followed by the orthogonal projection onto the subspace dictating the Toeplitz–Hankel structure in (5) (Line 9), then by a projection onto the γ_u-sphere (Lines 10–11), which is simply done by normalization. In Line 12, the projected $\boldsymbol{\Theta}$ is obtained. This loop iterates until convergence or until the maximum number of allowed iterations is reached.

3.2 Experiment application loop

Following the principles outlined in the beginning of this section, Algorithm 1 is integrated into the the main loop, which executes experiments in succession for system order estimation. This iterative scheme is presented in Algorithm 2.

Algorithm 2 iterates on the order of the system, starting at $r = 1$. The input is initialized such that Assumption 2.2 holds, and is applied on the real system (Line 2). The singular values from the data matrix $\mathbf{W}_L$ are then collected (line 3), and the main iteration begins. At every step of the iteration, a subspace identification method is applied on the data for the fixed order r (Line 5), and its resulting Markov parameters are used to build $\boldsymbol{F}$ via (5) (Line 6). Given the identified model of order r, Algorithm 1 is executed to obtain the input the maximizes the (Ln_u+r)-th singular value of $\mathbf{W}_L$ (Line 7). This input is tested in the real system (Line 8), and the new vector of singular values is computed (Line 9). Lines 10–13 provide the stopping criterion: in Line 10, the relative improvement in the (Ln_u+r)-th singular value of the real data matrix $\mathbf{W}_L$ is compared to a pre-established threshold; if the improvement is too low or negative, the model is falsified and the order is chosen to be $r-1$. Otherwise the loop continues by updating the singular values (Line 14) and incrementing r (Line 15).

4. NUMERICAL SIMULATION

To demonstrate the proposed method, we present two simulation studies. In the first part, we focus on the effectiveness of Algorithm 1 in increasing the singular value at the true cutoff index. In contrast, in the second part, the true system order is assumed to be unknown, and Algorithm 2 is executed to estimate the order. The

Algorithm 1 Optimal Input Design to Solve (6)

1: **function** `OptimalInput`($\boldsymbol{u}_{[0,N-1]}$,`Model`,$\boldsymbol{F}$,$\boldsymbol{\Pi}$,L,r,γ_u, η, ϵ_Θ)
2: $\quad k \leftarrow 1$
3: $\quad$ **repeat**
4: $\quad\quad \boldsymbol{\Theta} \leftarrow$ construct $\boldsymbol{\Theta}$ based on (5) using $\boldsymbol{u}_{[0,N-1]}$
5: $\quad\quad \boldsymbol{y}_{[0,N-1]} \leftarrow$ `Model`($\boldsymbol{u}_{[0,N-1]}$)
6: $\quad\quad \boldsymbol{q}_r,\, \boldsymbol{v}_r,\, \sigma_r \leftarrow \mathrm{SVD}\left(\mathbf{W}_L\right)$ $\quad$ ▷ based on (3)
7: $\quad\quad \nabla\ell_r \leftarrow \boldsymbol{F}^\mathsf{T}(\boldsymbol{q}_r\boldsymbol{v}_r^\mathsf{T})$
8: $\quad\quad \boldsymbol{\Theta}_{\text{new}} \leftarrow \boldsymbol{\Theta} + \frac{\eta}{\sqrt{k}}\nabla\ell_r$
9: $\quad\quad \boldsymbol{\Theta}_{\text{new}} \leftarrow \text{project}_{\boldsymbol{\Pi}^\perp}\, \mathrm{vec}(\boldsymbol{\Theta}_{\text{new}})$
10: $\quad\quad \boldsymbol{u}_{[0,N-1]} \leftarrow$ read off $\boldsymbol{u}_{[0,N-1]}$ from $\boldsymbol{\Theta}_{\text{new}}$
11: $\quad\quad \boldsymbol{u}_{[0,N-1]} \leftarrow \text{project}_{\mathcal{U}(\gamma_u)}\, \boldsymbol{u}_{[0,N-1]}$
12: $\quad\quad \boldsymbol{\Theta}_{\text{new}} \leftarrow$ construct $\boldsymbol{\Theta}$ based on (5) using $\boldsymbol{u}_{[0,N-1]}$
13: $\quad\quad k \leftarrow k+1$
14: $\quad$ **until** $\|\boldsymbol{\Theta}_{\text{new}} - \boldsymbol{\Theta}\| \leq \epsilon_\Theta$
15: $\quad \boldsymbol{u}^*_{[0,N-1]} \leftarrow \boldsymbol{u}_{[0,N-1]}$
16: **return** $\boldsymbol{u}^*_{[0,N-1]}$

Algorithm 2 Experimental Design for Order Estimation

Input: $\boldsymbol{u}_{[0,N-1]}$, $\boldsymbol{\Pi}$, L, γ_u, η, ϵ_Θ, ϵ_σ
Output: $\hat{n}$

$r \leftarrow 1$
$\boldsymbol{y}_{[0,N-1]} \leftarrow \texttt{System}(\boldsymbol{u}_{[0,N-1]})$ ▷ System (1)
$\sigma \leftarrow \text{SVD}\,(\mathbf{W}_L)$ ▷ based on (3)
while $r \leq Ln_y$ **do**
  $\{\boldsymbol{M}_i\}_{i=0}^{N-1}, \texttt{Model} \leftarrow \texttt{SysId}(\{\boldsymbol{u}_i, \boldsymbol{y}_i\}_{i=0}^{N-1}, r)$
  $\boldsymbol{F} \leftarrow$ construct $\boldsymbol{F}$ based on (5) using $\{\boldsymbol{M}_i\}_{i=0}^{N-1}$
  $\boldsymbol{u}_{[0,N-1]} \leftarrow \texttt{OptimalInput}(\boldsymbol{u}_{[0,N-1]}, \texttt{Model}, \boldsymbol{F}, \boldsymbol{\Pi}, L, Ln_u + r, \gamma_u, \eta, \epsilon_\Theta)$
  $\boldsymbol{y}_{[0,N-1]} \leftarrow \texttt{System}(\boldsymbol{u}_{[0,N-1]})$ ▷ System (1)
  $\sigma^{\text{new}} \leftarrow \text{SVD}\,(\mathbf{W}_L)$ ▷ based on (3)
  if $\sigma^{\text{new}}_{Ln_u+r} - \sigma_{Ln_u+r} \leq \epsilon_\sigma \sigma_{Ln_u+r}$ **then**
    $\hat{n} \leftarrow r - 1$
    return
  end if
  $\sigma \leftarrow \sigma^{\text{new}}$.
  $r \leftarrow r + 1$
end while

results in Figure 1 are obtained for the following stable LTI system:

$$\boldsymbol{A} = \begin{bmatrix} 2.8005 & -2.6973 & 0.8958 \\ 1 & 0 & 0 \\ 0 & 1 & 0 \end{bmatrix}, \; \boldsymbol{B} = \begin{bmatrix} 1 \\ 0 \\ 0 \end{bmatrix}$$
$$\boldsymbol{C} = [0.0194 \; -0.0366 \; 0.0182]\,, \; \boldsymbol{D} = \boldsymbol{0}\,,$$

which is the benchmark in the following sections.

4.1 Optimal Input Design

This study aims to show that a random input is not optimal for increasing the spectral gap, whereas an optimal input can excite the system in a desired manner. The optimization parameters are set as $N = 100$, $L = 13$, $\gamma_u = 1$,$\gamma_\Theta = 10^{-8}$, $\eta = 100$, with zero-mean i.i.d. Gaussian noise of variance $\varepsilon_e^2 = 10^{-7}$. The SNR level is approximately 20. The initial input is chosen as a bounded random Gaussian sequence with zero-mean and unit variance. The true order $n = 3$ is assumed to be known. The optimal input is designed based on the identified model via N4SID using Algorithm 1. The results, shown in Figure 2, clearly demonstrate a significant improvement in the spectral gap, that is, the singular value at $Ln_u + n$ increases by approximately 363% compared to the same singular value under a random input, while both inputs satisfy Assumption 2.2. This implies that the PE condition alone is not sufficient to guarantee a reliable identification process. Furthermore, the identification error can be assessed in multiple ways. Regarding the impulse response parameters $\boldsymbol{M}_i$, the optimal input reduces the error by about 70%. To evaluate the accuracy of $\text{col}(\mathbf{O}_L)$, we use principal angles to measure the distance between the subspaces, yielding a 13% improvement over a random input. Another noteworthy observation is the periodic nature of the optimal input, whose frequency content aligns with that of the underlying system. It is worth recalling that, in the optimization, no assumption is made regarding input periodicity beyond boundedness. To make the scenario more realistic, the next section assumes the true order is unknown and requires conducting experiments to determine the underlying order.

4.2 Robustness Evaluation

Maintain the same setup as in the previous section, but now assume that the true order $n = 3$ is not known in advance. In this situation, Algorithm 2 must be applied to determine the system order. Robustness is then assessed by conducting 200 experiments with distinct noise realizations. The confidence threshold ϵ_σ is chosen as 20%. The histogram of the estimated orders is shown in Figure 3a, and the results indicate a high level of accuracy of 90%. Figure 3b illustrates the evolution of the singular value growth for a given r at each trial. A sharp decline in the growth rate is evident at the true order at the true order $n = 3$ across the trials, which is consistent with the theoretical expectations.

5. CONCLUSION

Accurately identifying the true system order is directly linked to the quality of system identification. For this reason, we have proposed an iterative approach to determine the order that best explains the perturbed data. This approach is enabled through an optimal input design that maximizes a particular singular value associated with a low-rank data representation, thereby making the system information more distinguishable from noise. Since our optimal input design depends only on the identified model rather than the true system, it leads to a minimal number of experiments required for estimation. We would like to stress that, despite being presented as an algorithm, our method serves as a guideline for experiment design; e.g., inspecting the relative improvements in singular value over a range of orders a posteriori may be beneficial. Future work will be dedicated to the problem of minimizing the number of experiments by using, e.g., bisection instead of linear search over r, and determining guarantees of the proposed method.

DECLARATION OF GENERATIVE AI AND AI-ASSISTED TECHNOLOGIES IN THE WRITING PROCESS

During the preparation of this work the author(s) did not use any generative AI technology.

REFERENCES

Aoki, M. and Staley, R. (1970). On input signal synthesis in parameter identification. *Automatica*, 6(3), 431–440.

Bombois, X., Gevers, M., Hildebrand, R., and Solari, G. (2011). Optimal experiment design for open and closed-loop system identification. *Commun. Inf. Syst.*, 11(3), 197–224. doi:10.4310/CIS.2011.v11.n3.a1.

Coulson, J., Van Waarde, H.J., Lygeros, J., and Dörfler, F. (2022). A quantitative notion of persistency of excitation and the robust fundamental lemma. *IEEE Control Systems Letters*, 7, 1243–1248.

Dirkx, N., van de Wijdeven, J., and Oomen, T. (2020). Frequency response function identification for multivariable motion control: Optimal experiment design with element-wise constraints. *Mechatronics*, 71, 102440.

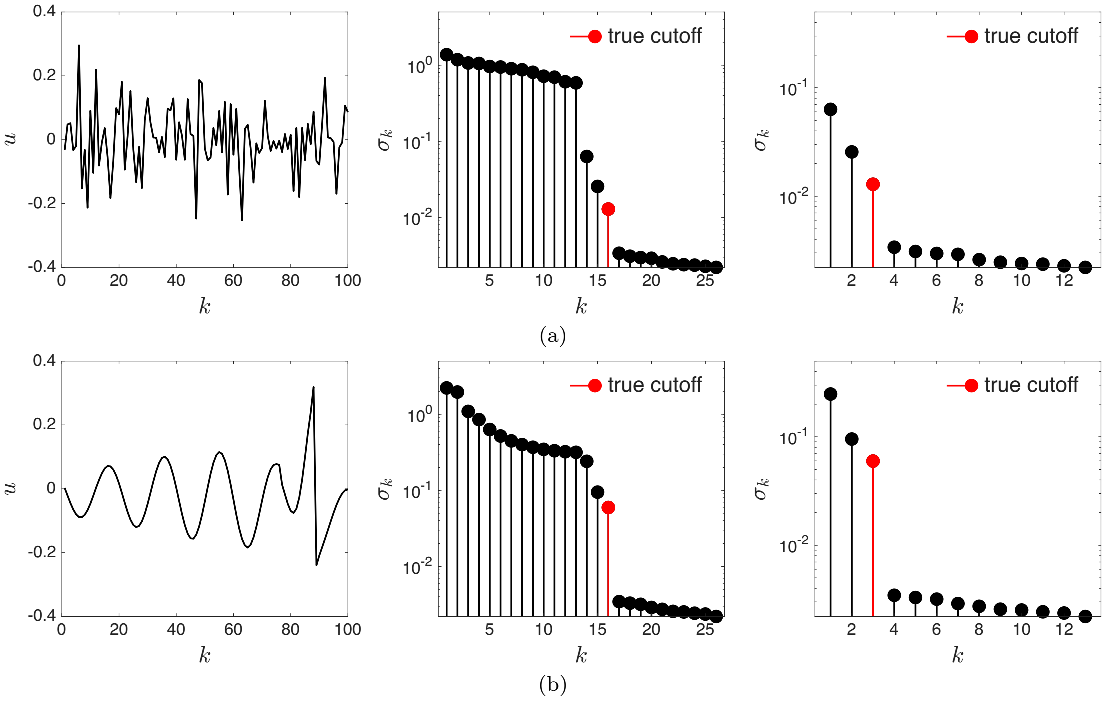

Fig. 2. This figure compares the performance of random and optimal inputs. Part (a) shows the results for the initial random input, while part (b) presents those for the optimal input. From left to right, the plots display the input signal, the $\mathbf{W}_L$ singular values, and the MOESP singular values. The red circle marks the true cutoff, with its position depends on the method used.

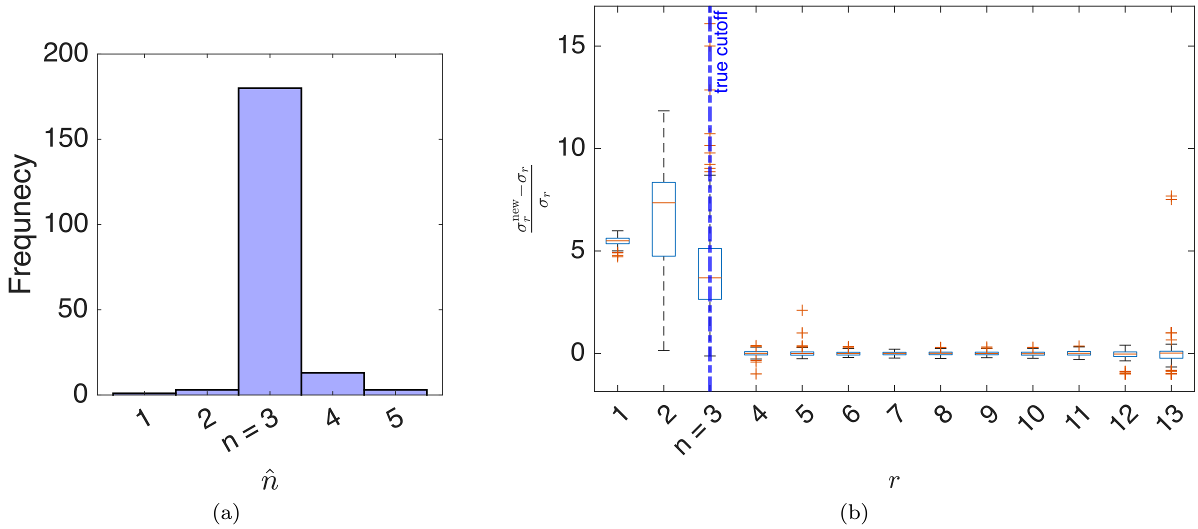

Fig. 3. Panel (a) illustrates the histogram of system order estimation using Algorithm 2, while Panel (b) shows the box plot of the singular value growth rate for each r across all trials.

Goodwin, G. (1971). Optimal input signals for nonlinear-system identification. In *Proc. IEE*, volume 118, 922–926.

Lewis, A.S. and Sendov, H.S. (2005). Nonsmooth analysis of singular values. part i: Theory. *Set-Valued Analysis*, 13(3), 213–241.

Lindqvist, K. and Hjalmarsson, H. (2001). Identification for control: adaptive input design using convex optimization. In *Proceedings of the 40th IEEE Conference on Decision and Control (Cat. No.01CH37228)*, volume 5, 4326–4331 vol.5. doi:10.1109/CDC.2001.980881.

Ljung, L. (1998). System identification. In *Signal analysis and prediction*, 163–173. Springer.

Mehra, R. (1974). Optimal inputs for linear system identification. *IEEE Trans. Autom. Control*, 19(3), 192–200.

Misra, S. and Nikolaou, M. (2017). Adaptive design of experiments for model order estimation in subspace identification. *Computers & Chemical Engineering*, 100, 119–138.

Van Overschee, P. and De Moor, B. (1994). N4sid: Subspace algorithms for the identification of combined deterministic-stochastic systems. *Automatica*, 30(1),

75–93.
Verhaegen, M. and Dewilde, P. (1992). Subspace model identification part 2. analysis of the elementary output-error state-space model identification algorithm. *International journal of control*, 56(5), 1211–1241.
Verhaegen, M. and Verdult, V. (2007). *Filtering and system identification: a least squares approach*. Cambridge university press.
Wagenmaker, A. and Jamieson, K. (2020). Active learning for identification of linear dynamical systems. In *Conference on Learning Theory*, 3487–3582. PMLR.
Willems, J.C., Rapisarda, P., Markovsky, I., and De Moor, B.L. (2005). A note on persistency of excitation. *Systems & Control Letters*, 54(4), 325–329.
Yu, Y., Talebi, S., Van Waarde, H.J., Topcu, U., Mesbahi, M., and Açıkmeşe, B. (2021). On controllability and persistency of excitation in data-driven control: Extensions of willems' fundamental lemma. In *2021 60th IEEE Conference on Decision and Control (CDC)*, 6485–6490. IEEE.